



Cite this: *Chem. Commun.*, 2016, 52, 12765

Received 18th August 2016,  
Accepted 29th September 2016

DOI: 10.1039/c6cc06786g

www.rsc.org/chemcomm

## Hydrothermal synthesis of high silica zeolite Y using tetraethylammonium hydroxide as a structure-directing agent†

Dawei He,<sup>‡,ab</sup> Danhua Yuan,<sup>‡,a</sup> Zhijia Song,<sup>ab</sup> Yansi Tong,<sup>ab</sup> Yaqi Wu,<sup>ab</sup> Shutao Xu,<sup>a</sup> Yunpeng Xu<sup>\*a</sup> and Zhongmin Liu<sup>\*a</sup>

**High silica zeolite Y with a SiO<sub>2</sub>/Al<sub>2</sub>O<sub>3</sub> ratio of 7.76 is successfully synthesized with tetraethylammonium hydroxide (TEAOH) as a structure-directing agent. The high silica zeolite Y shows outstanding high temperature thermal stability and hydrothermal stability.**

Zeolite Y, one of the most important members in the zeolite family, has been widely used as a fluidized catalytic cracking (FCC) catalyst.<sup>1–4</sup> As a typical aluminosilicate zeolite, the SiO<sub>2</sub>/Al<sub>2</sub>O<sub>3</sub> ratio of zeolite Y has an important effect on its thermal and hydrothermal stability. Industrial practices and related studies reveal that high silica zeolite Y exhibits outstanding catalytic activity and hydrothermal stability.<sup>5–7</sup> To date, high silica zeolite Y used in the FCC process has been mainly produced by the post-synthesis method. However, the post-synthesis method is complicated, highly energy consuming and environmentally unfriendly. Therefore, it is of great significance to develop a direct and clean synthesis method for high silica zeolite Y.

In 1990, Delprato *et al.* directly synthesized high silica zeolite Y with a SiO<sub>2</sub>/Al<sub>2</sub>O<sub>3</sub> ratio of around 9 by employing 15-Crown-5 as a structure directing agent (SDA).<sup>8</sup> Their work revealed a one-step simple way for the synthesis of high silica zeolite Y. Nevertheless, the high cost and toxicity of crown ethers limited its industrial applications.<sup>9,10</sup> After that, lots of efforts have been made in developing nontoxic and inexpensive organic SDAs to synthesize high silica zeolite Y, such as poly(ethylene oxides), inositol, *N*-methylpyridinium iodide and 1-ethyl(butyl)-3-methylimidazolium bromide, which all have been successfully used to synthesize high silica zeolite Y with a SiO<sub>2</sub>/Al<sub>2</sub>O<sub>3</sub> ratio of 6–7.<sup>11–14</sup> However, zeolite Y with a SiO<sub>2</sub>/Al<sub>2</sub>O<sub>3</sub> ratio higher than 7 is hardly achieved by the one-step synthesis method without using crown ethers as SDAs.

Tetraethylammonium hydroxide, a commonly used SDA, has been employed in the synthesis of zeolites such as Beta, ZSM-20, and SAPO-34.<sup>15–17</sup> Among them, the structure of ZSM-20 is an intergrowth mixture of the cubic FAU framework and EMT topology.<sup>18</sup> In the present work, high silica zeolite Y with pure FAU topology is successfully synthesized by using TEAOH as an organic SDA. The highest SiO<sub>2</sub>/Al<sub>2</sub>O<sub>3</sub> ratio of the samples reaches 7.76, which is much higher than the results of most organic SDAs except crown ethers. The effects of Na<sup>+</sup> and TEA<sup>+</sup> on the synthesis of high silica zeolite Y are investigated. It is found that the TEA<sup>+</sup>/Na<sup>+</sup> ratio of the starting gel has a strong relationship with the SiO<sub>2</sub>/Al<sub>2</sub>O<sub>3</sub> ratio of zeolite Y. In addition, we observed MOR–FAU–BEA phase transformation by changing the relative amounts of TEAOH and NaOH in the synthesis gel.

We synthesized a series of samples by using TEAOH as an organic SDA after crystallization at 120 °C for a few days. Among them, TEA-1 has the highest SiO<sub>2</sub>/Al<sub>2</sub>O<sub>3</sub> ratio with a pure FAU framework. The XRD pattern indicates that the typical peaks of TEA-1 are associated with those of FAU topology (Fig. 1A).

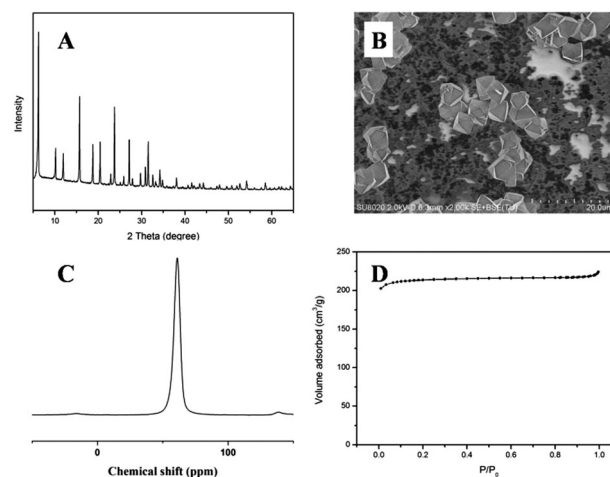


Fig. 1 (A) XRD pattern of the as-synthesized sample TEA-1. (B) SEM image of the sample TEA-1. (C) <sup>27</sup>Al-NMR spectrum of the sample TEA-1. (D) N<sub>2</sub> sorption isotherm of the sample TEA-1.

<sup>a</sup> National Engineering Laboratory for Methanol to Olefins, Dalian National Laboratory for Clean Energy, Dalian Institute of Chemical Physics, Chinese Academy of Sciences, Dalian 116023, P. R. China. E-mail: xuyy@dicp.ac.cn, liuzm@dicp.ac.cn

<sup>b</sup> University of Chinese Academy of Sciences, Beijing 100049, P. R. China

† Electronic supplementary information (ESI) available: Experimental and characterization details, XRD patterns, and TG–DSC curves. See DOI: 10.1039/c6cc06786g

‡ These authors contributed equally to this work.

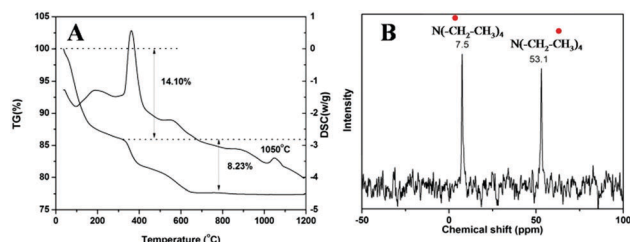


**Fig. 2** (A) TG–DSC curves of the as-synthesized sample TEA-1. TG–DSC analysis is carried out from room temperature to 1200 °C in an air flow of 100 ml min<sup>-1</sup>. The weight loss with endothermic peaks at 100–300 °C is attributed to the water desorption from zeolites. The weight loss with exothermic peaks at 300–800 °C is due to the decomposition of organic templates. The exothermic peaks above the temperature of 800 °C are attributed to the structural collapse of zeolite Y. (B) <sup>13</sup>C-NMR spectrum of the as-synthesized sample TEA-1.

The SEM image shows that TEA-1 has uniform octahedral particles and the average particle size is approximately 5–6 μm (Fig. 1B). The <sup>27</sup>Al MAS-NMR spectrum of TEA-1 shows that only one pointed peak is displayed at about 60 ppm, which is assigned to tetrahedral-coordinated aluminium species in the framework (Fig. 1C). After calcination at 550 °C for 4 h, the N<sub>2</sub> adsorption-desorption isotherm of TEA-1 is a typical type-I sorption isotherm, corresponding to the apparent microporous character of the zeolite (Fig. 1D). These characterization results indicate that the product TEA-1 is highly crystalline zeolite Y without any impurity.

Fig. 2A shows the TG/DSC curves of the sample TEA-1. The main exothermic peaks at 200–700 °C, accompanied by a weight loss of about 8.23%, are attributed to the decomposition of organic templates. The carbon content of TEA-1 calculated by the TOC method is 6.78%, and the Na<sub>2</sub>O/Al<sub>2</sub>O<sub>3</sub> ratio of the sample TEA-1 (0.78) is much lower than that of the Na-Y sample (0.98) as tested by XRF, Table 1. The <sup>13</sup>C-NMR spectrum of the sample TEA-1 is shown in Fig. 2B. The peaks at 53.1 ppm and 7.5 ppm are nearly assigned to the N–CH<sub>2</sub>– and –CH<sub>3</sub> groups of tetraethylammonium hydroxide respectively.<sup>19,20</sup> These results suggest that there is a certain amount of organic templates presented in the sample and TEA<sup>+</sup> is basically stable in the zeolite framework during the synthesis.

Among the abundant synthesized samples, some samples with good crystallinity are shown in Table 1. It presents the effect of the TEA<sup>+</sup>/Na<sup>+</sup> ratio of the starting gel on the SiO<sub>2</sub>/Al<sub>2</sub>O<sub>3</sub> ratio of zeolite Y. The SiO<sub>2</sub>/Al<sub>2</sub>O<sub>3</sub> ratios of the products are

obtained by <sup>29</sup>Si-NMR, XRF and ICP. The XRF results show that the samples (TEA-1, 2, 3, 4) prepared using TEAOH as an SDA have high SiO<sub>2</sub>/Al<sub>2</sub>O<sub>3</sub> ratios of 7.0–7.7, which are much higher than that of the product Na-Y synthesized without organic SDAs (5.79). When the TEA<sup>+</sup>/Na<sup>+</sup> ratios increase from 0.33 to 1.15 in their starting gels, the SiO<sub>2</sub>/Al<sub>2</sub>O<sub>3</sub> ratios of the products increase from 7.08 to 7.76 calculated using XRF results (6.75 to 7.26 using <sup>29</sup>Si-NMR results) in Table 1. The ICP results are also in a good agreement with the variation trend that the SiO<sub>2</sub>/Al<sub>2</sub>O<sub>3</sub> ratios of the products increase as the TEA<sup>+</sup>/Na<sup>+</sup> ratios increase in their starting gels. Furthermore, the features of the as-synthesized samples are characterized in the <sup>29</sup>Si-NMR spectrum (Fig. 3). The peaks of Si(0Al) and Si(1Al) species are significantly strengthened, and the peaks of Si(2Al) and Si(3Al) species are accordingly weakened from TEA-4 to TEA-1. It is concluded that the high TEA<sup>+</sup>/Na<sup>+</sup> ratio in the starting gel is helpful for enhancing the SiO<sub>2</sub>/Al<sub>2</sub>O<sub>3</sub> ratio of zeolite Y.

XRF, ICP and TOC results also show that the mass fraction of TEA<sup>+</sup> in as-synthesized samples increases with an increase in the TEA<sup>+</sup>/Na<sup>+</sup> ratio of the starting gels, Table 1. It could be inferred that as the TEA<sup>+</sup>/Na<sup>+</sup> ratio in the starting gel increases, more tetraethylammonium ions are incorporated into the FAU framework and partially replace sodium ions to balance the negative charge of the framework.

In addition, it is found that the TEA<sup>+</sup>/Na<sup>+</sup> and OH<sup>-</sup>/Al ratios of the starting gel have strong effects on the structures of products in Fig. 4. We observed the phase transformation of products when the TEA<sup>+</sup>/Na<sup>+</sup> and OH<sup>-</sup>/Al ratios were changed. When the OH<sup>-</sup>/Al ratio was 1.6, the crystallization of zeolites had been suppressed extensively and all the products were still amorphous structures after 14 days of crystallization. As the OH<sup>-</sup>/Al ratios were increased to 1.8–2.0, MOR–FAU–BEA phase transformation was observed when the TEA<sup>+</sup>/Na<sup>+</sup> ratio of the starting gels was increased gradually. It could be inferred that a high TEAOH/NaOH ratio is helpful for the generation of BEA, whereas the formation of MOR requires a high NaOH content.<sup>21,22</sup> However, only a FAU–GIS binary mixture could be obtained as the OH<sup>-</sup>/Al ratios increased to 2.2. The SEM images of FAU, FAU/GIS, FAU/MOR and FAU/BEA phases are shown in Fig. 5. Pure and highly crystalline FAU zeolites could be synthesized within a narrow region: TEA<sup>+</sup>/Na<sup>+</sup> ratios of 0.32–1.25, and OH<sup>-</sup>/Al ratios of 1.8–2.0.

It is well known that high silica zeolite Y shows outstanding high temperature thermal stability and hydrothermal stability,

**Table 1** Compositions of the starting gels, SiO<sub>2</sub>/Al<sub>2</sub>O<sub>3</sub> ratios and Na<sub>2</sub>O/Al<sub>2</sub>O<sub>3</sub> ratios of the as-synthesized products

Sample	Na <sub>2</sub> O/TEA <sub>2</sub> O/ SiO <sub>2</sub> /Al <sub>2</sub> O <sub>3</sub> /H <sub>2</sub> O	Relative crystallinity <sup>a</sup> (%)	SiO <sub>2</sub> /Al <sub>2</sub> O <sub>3</sub> ratio of products			Na <sub>2</sub> O/Al <sub>2</sub> O <sub>3</sub> ratio of products		Carbon content TOC <sup>e</sup> (%)
			XRF <sup>b</sup>	ICP <sup>c</sup>	<sup>29</sup> Si-NMR <sup>d</sup>	XRF <sup>b</sup>	ICP <sup>c</sup>	
TEA-1	1.3/1.5/10/1/90	100	7.76	7.53	7.26	0.78	0.65	6.78
TEA-2	1.5/1.3/10/1/90	91.1	7.44	—	6.96	0.82	—	5.55
TEA-3	1.8/1.0/10/1/90	97.6	7.24	—	6.84	0.84	—	4.99
TEA-4	2.1/0.7/10/1/90	78.3	7.08	7.00	6.75	0.87	0.78	4.04
Na-Y	3.2/0.0/10/1/90	81.1	5.79	5.51	5.64	0.98	0.95	—

All the above as-synthesized products are pure FAU phases with good crystallinity. The XRD patterns of these samples are shown in Fig. S1 (ESI).<sup>a</sup> Relative crystallinity of the samples is calculated based on TEA-1. <sup>b</sup> SiO<sub>2</sub>/Al<sub>2</sub>O<sub>3</sub> ratios and Na<sub>2</sub>O/Al<sub>2</sub>O<sub>3</sub> ratios obtained by XRF. <sup>c</sup> SiO<sub>2</sub>/Al<sub>2</sub>O<sub>3</sub> ratios and Na<sub>2</sub>O/Al<sub>2</sub>O<sub>3</sub> ratios obtained by ICP. <sup>d</sup> SiO<sub>2</sub>/Al<sub>2</sub>O<sub>3</sub> ratios obtained by <sup>29</sup>Si-NMR. <sup>e</sup> The carbon content obtained by TOC (total organic carbon) analysis.

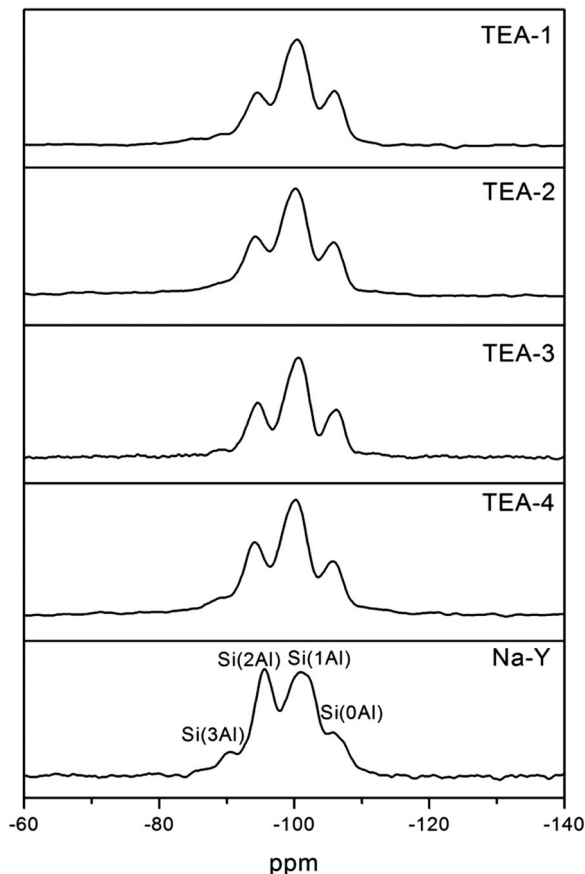


Fig. 3  $^{29}\text{Si}$ -NMR spectra of the samples TEA-1, TEA-2, TEA-3, TEA-4 and Na-Y.

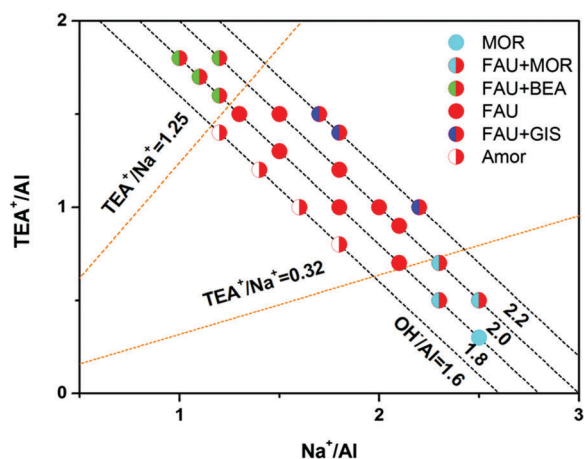


Fig. 4 Two-dimensional phase diagram of samples prepared with different compositions. Each data point corresponds to crystals synthesized with the same raw materials at 120 °C. The composition of the starting gels is  $x\text{Na}_2\text{O}/y\text{TEA}_2\text{O}/10\text{SiO}_2/1\text{Al}_2\text{O}_3/90\text{H}_2\text{O}$ . The specific data of these samples are shown in Table S1 (ESI $^\dagger$ ). The  $\text{TEA}^+/\text{Na}^+$  ratio in the starting gels is indicated by orange imaginary lines. The  $\text{OH}^-$  content in the starting gels is indicated by black imaginary lines, which is calculated by the sum of TEAOH and NaOH content.

which are crucial factors for industrial applications. As shown in Fig. 2B and Fig. S2 (ESI $^\dagger$ ), the TG–DSC curves show that Na-Y

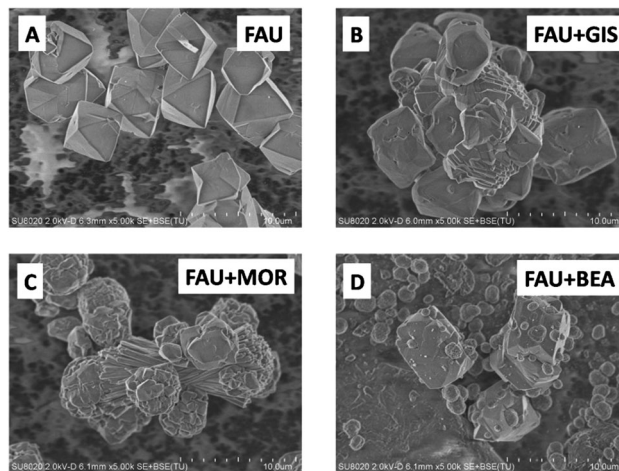


Fig. 5 SEM images of the (A) FAU phase, (B) FAU/GIS phase, (C) FAU/MOR phase, and (D) FAU/BEA phase.

starts to collapse at 950 °C, but TEA-1 remains stable until 1050 °C. The collapse temperature of HTEA-1 and HNa-Y (H-form TEA-1 and Na-Y) has declined slightly to 1046 °C and 936 °C, respectively (Fig. S3, ESI $^\dagger$ ). It is concluded that TEA-1 has higher thermal stability than the Na-Y sample. The hydrothermal stability analysis also displays that HTEA-1 is more stable than HNa-Y (Fig. 6). After 100% steam treatment at 750 °C for 2 h, the crystallinity of zeolite Y was contributed by the coordination states of Si and Al in its framework.<sup>23,24</sup> Compared with the sample Na-Y, the content of aluminium atoms in the tetrahedral coordination of  $\text{SiO}_4$  species in sample TEA-1 is substantially reduced, and the framework's  $\text{SiO}_2/\text{Al}_2\text{O}_3$  ratio increases accordingly (Fig. 3). The results indicate that TEA-1 has more silicon–oxygen–silicon bonds than that of NaY, which is beneficial to its thermal stability and hydrothermal stability.

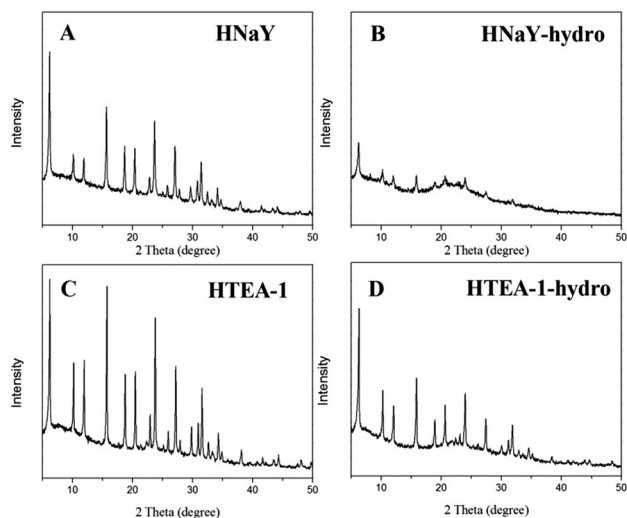


Fig. 6 XRD patterns of (A) HNa-Y, (B) HNa-Y-hydro, (C) HTEA-1 and (D) HTEA-1-hydro. HNa-Y-hydro and HTEA-1-hydro, respectively, correspond to HNa-Y and HTEA-1 after 100% steam treatment at 750 °C for 2 h.

In conclusion, highly crystalline zeolite Y with a SiO<sub>2</sub>/Al<sub>2</sub>O<sub>3</sub> ratio of higher than 7 is synthesized with TEOH as an organic SDA. Pure FAU zeolite is synthesized within a narrow region of the TEA<sup>+</sup>/Na<sup>+</sup> ratio and the OH<sup>-</sup>/Al ratio in the starting gel. We could observe MOR-FAU-BEA phase transformation with the variations of TEA<sup>+</sup>/Na<sup>+</sup> in the starting gels. Moreover, it is found that the TEA<sup>+</sup>/Na<sup>+</sup> ratio of the starting gels has an important effect on the SiO<sub>2</sub>/Al<sub>2</sub>O<sub>3</sub> ratio of the products. The highest SiO<sub>2</sub>/Al<sub>2</sub>O<sub>3</sub> ratio of the samples could reach 7.76. Compared with conventional zeolite Y synthesized without organic SDAs, Y zeolites synthesized with TEOH as an SDA have remarkably higher SiO<sub>2</sub>/Al<sub>2</sub>O<sub>3</sub> ratios and exhibit outstanding hydrothermal stability and thermal stability. These features are of great significance for the future industrial application of high silica Y zeolite as the FCC catalyst.

## Notes and references

- M. E. Davis and R. F. Lobo, *Chem. Mater.*, 1992, **4**, 756–768.
- J. Scherzer, *Appl. Catal.*, 1991, **75**, 1–32.
- S. Babitz, B. Williams, J. Miller, R. Snurr, W. Haag and H. Kung, *Appl. Catal., A*, 1999, **179**, 71–86.
- P. T. M. Do, J. R. McAtee, D. A. Watson and R. F. Lobo, *ACS Catal.*, 2013, **3**, 41–46.
- M. A. Cambor, A. Corma, A. Martínez, F. A. Mocholí and J. P. Pariente, *Appl. Catal.*, 1989, **55**, 65–74.
- B. Xu, S. Bordiga, R. Prins and J. A. van Bokhoven, *Appl. Catal., A*, 2007, **333**, 245–253.
- B. Williams, S. Babitz, J. Miller, R. Snurr and H. Kung, *Appl. Catal., A*, 1999, **177**, 161–175.
- F. Delprato, L. Delmotte, J. L. Guth and L. Huve, *Zeolites*, 1990, **10**, 546–552.
- T. Chatelain, J. Patarin, M. Soulard, J. Guth and P. Schulz, *Zeolites*, 1995, **15**, 90–96.
- K. Karim, J. Zhao, D. Rawlence and J. Dwyer, *Microporous Mater.*, 1995, **3**, 695–698.
- D. Yuan, D. He, S. Xu, Z. Song, M. Zhang, Y. Wei, Y. He, S. Xu, Z. Liu and Y. Xu, *Microporous Mesoporous Mater.*, 2015, **204**, 1–7.
- F. Dougnier, J. Patarin, J. L. Guth and D. Anglerot, *Zeolites*, 1993, **13**, 122–127.
- B. De Witte, J. Patarin, D. Le Nouen, L. Delmotte, J. L. Guth and T. Cholley, *Microporous Mesoporous Mater.*, 1998, **23**, 11–22.
- L. Zhu, L. Ren, S. Zeng, C. Yang, H. Zhang, X. Meng, M. Rigutto, A. van der Made and F.-S. Xiao, *Chem. Commun.*, 2013, **49**, 10495–10497.
- M. Cambor, A. Mifsud and J. Pérez-Pariente, *Zeolites*, 1991, **11**, 792–797.
- S. Ernst, G. T. Kokotailo and J. Weitkamp, *Zeolites*, 1987, **7**, 180–182.
- R. Vomscheid, M. Briend, M. Peltre, P. Man and D. Barthomeuf, *J. Phys. Chem.*, 1994, **98**, 9614–9618.
- J. M. Newsam, M. M. J. Treacy, D. E. W. Vaughan, K. G. Strohmaier and W. J. Mortier, *J. Chem. Soc., Chem. Commun.*, 1989, 493–495.
- Y. Shi, E. Xing, W. Xie, F. Zhang, X. Mu and X. Shu, *Appl. Catal., A*, 2015, **497**, 135–144.
- D. J. Evans, G. J. Leigh and C. J. Macdonald, *Magn. Reson. Chem.*, 1990, **28**, 711–714.
- M. A. Cambor and J. Perezpariente, *Zeolites*, 1991, **11**, 202–210.
- G. J. Kim and W. S. Ahn, *Zeolites*, 1991, **11**, 745–750.
- G. T. Kerr, *J. Phys. Chem.*, 1968, **72**, 2594–2596.
- G. T. Kerr, *J. Phys. Chem.*, 1969, **73**, 2780–2782.